Electronic Supplementary Material (ESI) for RSC Advances.

Composition controlled nickel cobalt sulfides core-shell structure as high capacity and good rate-capability electrodes for hybrid supercapacitors

Lei Zhang,[+] Haitao Zhang,[+,*] Long Jin, Binbin Zhang, Fangyan Liu, Hai Su, Fengjun Chun, Qinghan Li, Jinfang Peng, Weiqing Yang *

Key Laboratory of Advanced Technologies of Materials (Ministry of Education), School of Materials Science and Engineering, Southwest Jiaotong University, Chengdu 610031, China.

*To whom correspondence should be addressed. E-mail: wqyang@swjtu.edu.cn, haitaozhang@swjtu.edu.cn.

[+] These authors contributed equally to this work.

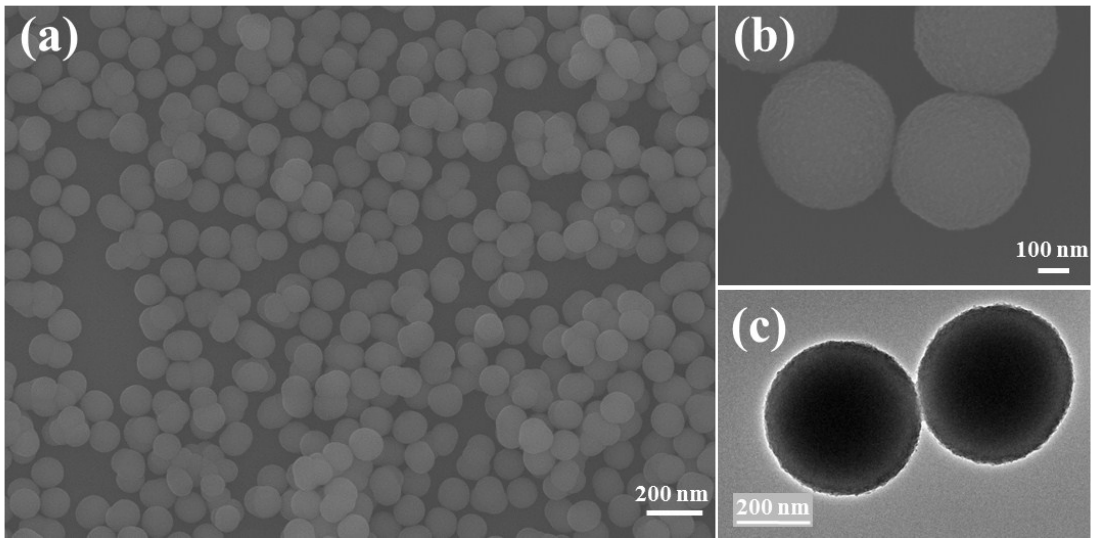

Figure S1. The morphology of the precursors NiCo-glycerate spheres corresponding to the $NiCo_2S_4$ sample. (a, b) FESEM image. (c) TEM image.

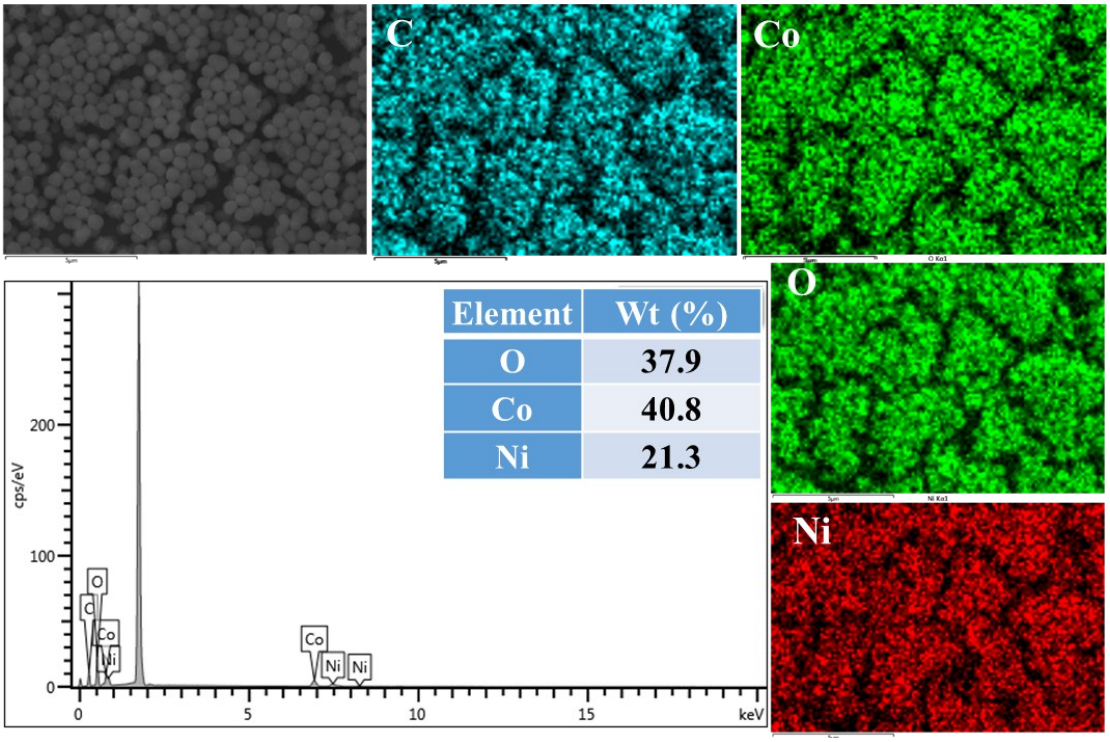

Figure S2. SEM image and EDS-elemental mapping images of NiCo-glycerate spheres corresponding to the $NiCo_2S_4$ sample.

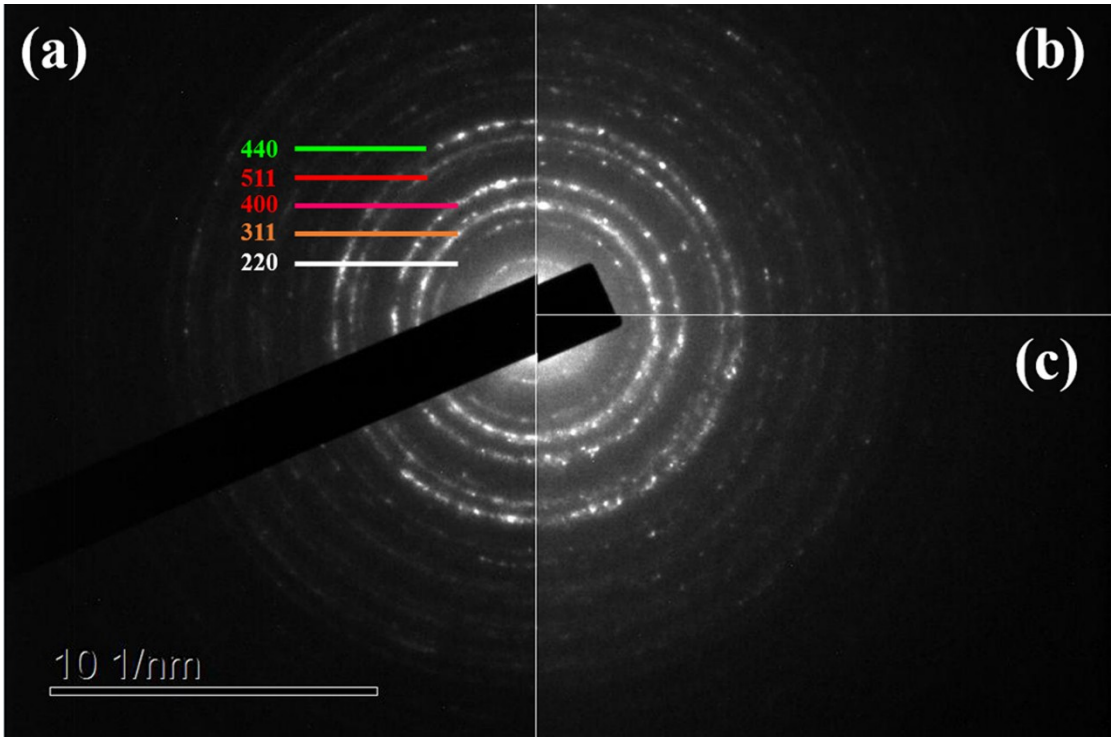

Figure S3. The SAED patterns of the Ni–Co sulfides: (a) $NiCo_2S_4$, (b) $Ni_{1.5}Co_{1.5}S_4$, and (c) Ni_2CoS_4, respectively.

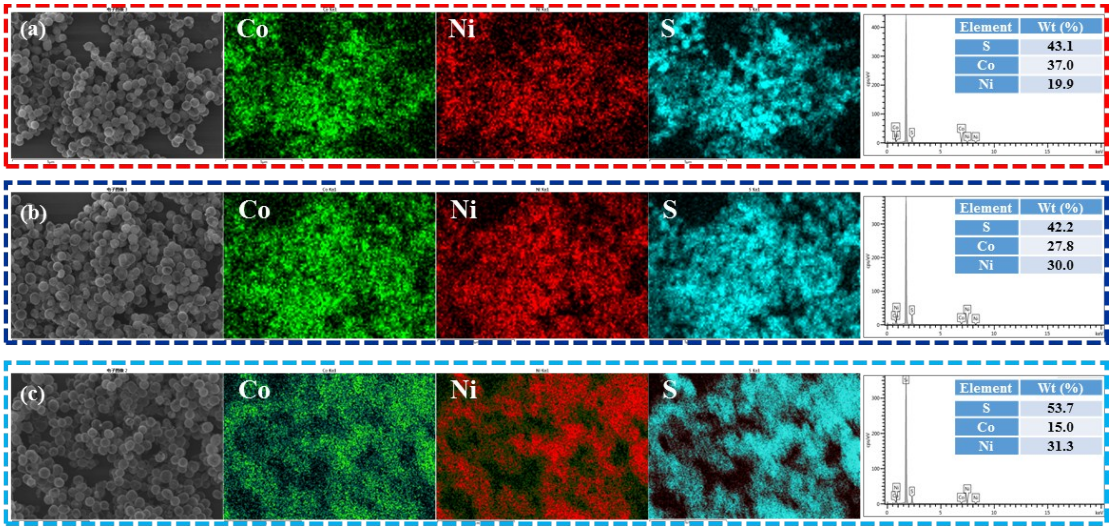

Figure S4. SEM-EDS elemental mapping images and its corresponding EDS spectra: (a) $NiCo_2S_4$, (b) $Ni_{1.5}Co_{1.5}S_4$, and (c) Ni_2CoS_4.

Table S1. The ratio of nickel and cobalt according to their XPS data.

Element	*Ni At (%)*	*Co At (%)*	$R_{Ni/Co}$
$NiCo_2S_4$	35.1	64.9	1/1.9
$Ni_{1.5}Co_{1.5}S_4$	47.2	52.8	1/1.1
Ni_2CoS_4	65.4	34.6	1.9/1

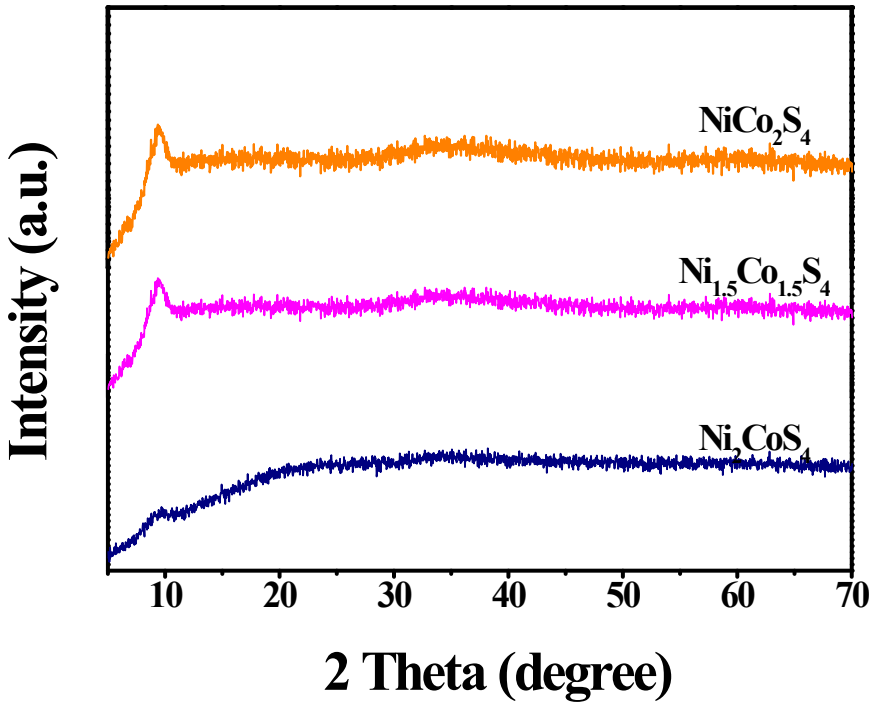

Figure S5. XRD patterns of the NiCo-glycerate precursor of $NiCo_2S_4$, $Ni_{1.5}Co_{1.5}S_4$, and Ni_2CoS_4.

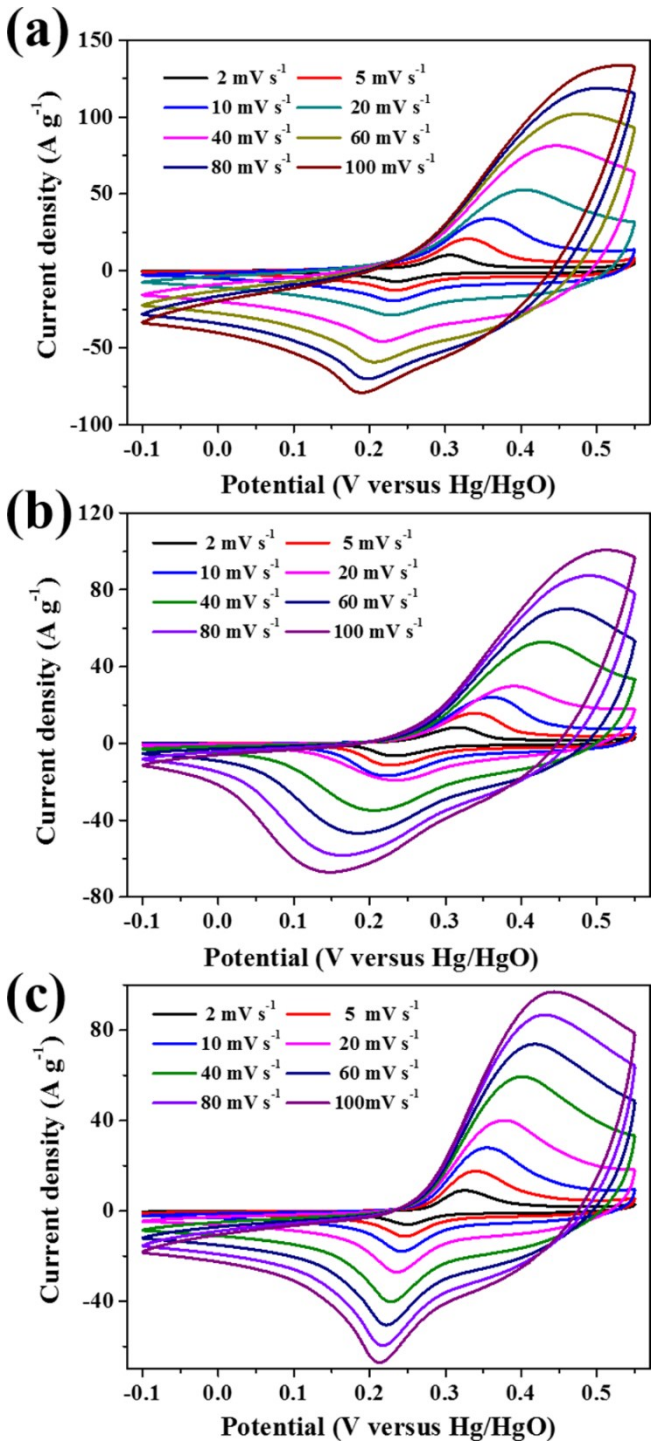

Figure S6. The cyclic voltammetry curves with the scan rate ranging from 2 to 100 mV s^{-1} of (a) $NiCo_2S_4$, (b) $Ni_{1.5}Co_{1.5}S_4$, and (c) Ni_2CoS_4.

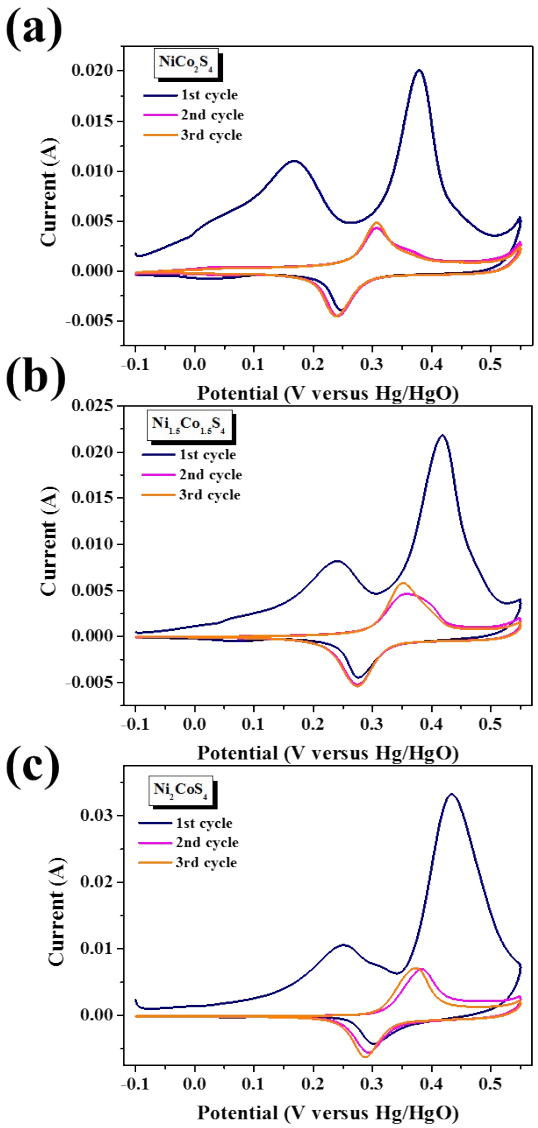

Figure S7. The first three CV curves at 0.5 mV $s^{-1}$of (a) $NiCo_2S_4$, (b) $Ni_{1.5}Co_{1.5}S_4$ and (c) Ni_2CoS_4. Both of the samples are full immerged into 6M KOH solution overnight and tested with a fresh electrode.

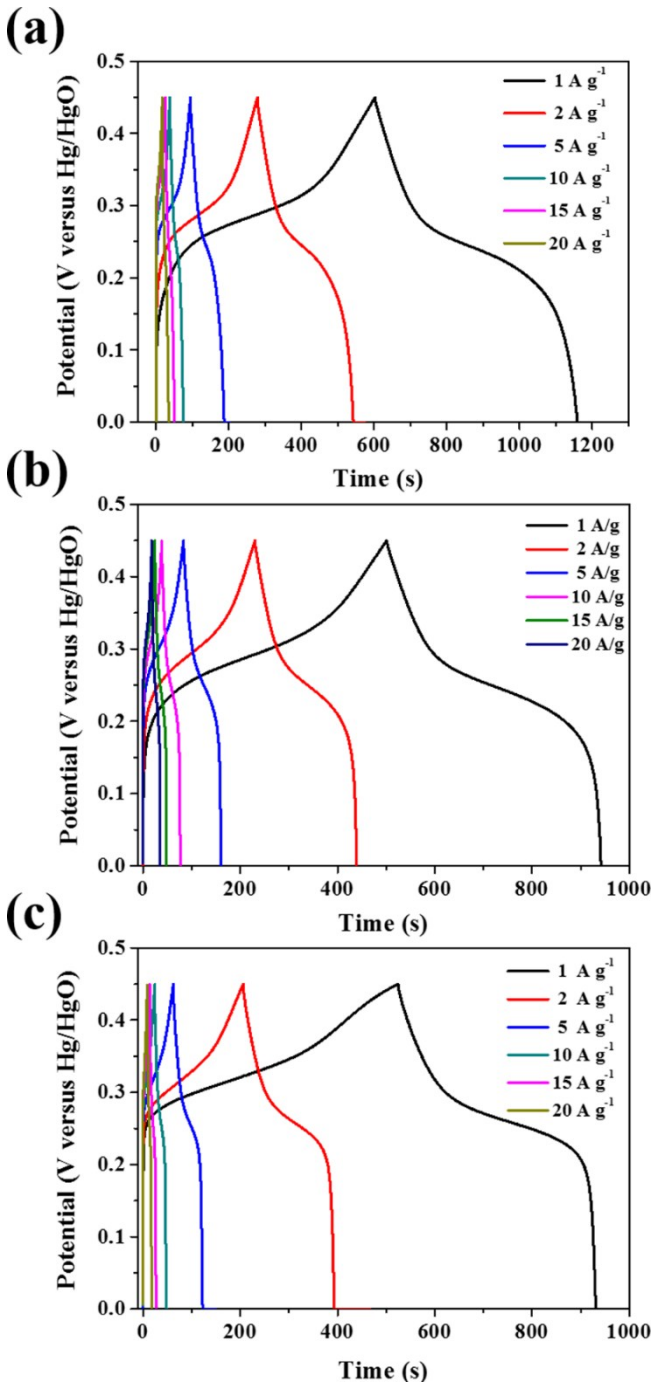

Figure S8. The galvanostatic charging/discharging voltage profiles with the current density ranging from 1 to 20 A g^{-1} of (a) $NiCo_2S_4$, (b) $Ni_{1.5}Co_{1.5}S_4$, and (c) Ni_2CoS_4.

Table S2. Rate capacity of Ni−Co sulfide with different micro/nano structure from recent reports in three electrode configuration.

Reference	Micro/nano structure	Capacity	Specific capacity	Capacity retention
This work	Core-shell sphere ($Ni_{1.5}Co_{1.5}S_4$)	122 mAh g^{-1} (1 A g^{-1})	98 mAh g^{-1} (20 Ag^{-1})	**80**% from 1 to 20 A g^{-1}
1	Mesoporous nanosheet	124 mAh g^{-1} (1 A g^{-1})	103 mAh g^{-1} (20 Ag^{-1})	**83.3**% from 1 to 20 A g^{-1}
2	Nanosheet	173 mAh g^{-1} (1 A g^{-1})	705 mAh g^{-1} (20 Ag^{-1})	**68**% from 1 to 20 A g^{-1}
3	Hollow tubular syructure	159 mAh g^{-1} (2 A g^{-1})	108 mAh g^{-1} (20 Ag^{-1})	**68**% from 2 to 20 A g^{-1}
4	Hollow nanoneedle arrays on carbon fiber paper	208 mAh g^{-1} (1 A g^{-1})	129 mAh g^{-1} (20 A g^{-1})	**62**% from 1 to 20 A g^{-1}
5	Hollow nanoprism	136 mAh g^{-1} (1 A g^{-1})	89 mAh g^{-1} (20 Ag^{-1})	**65**% from 1 to 20 A g^{-1}
6	$NiCo_2S_4/Ni(OH)_2$ core-shell heterostructured nanotube arrays on carbon-fabric	450 mAh g^{-1} (1 mA cm^{-2})	266 mAh g^{-1} (20 mA cm^{-2})	**59%** from 1 to 20 mA cm^{-2}
7	Nanotube array	302 mAh g^{-1} (3 A g^{-1})	158 mAh g^{-1} (20 Ag^{-1})	**52**% from 3 to 20 A g^{-1}
8	Hollow hexagonal	48 mAh g^{-1} (1 A g^{-1})	25 mAh g^{-1} (20 Ag^{-1})	**53**% from 1 to 20 A g^{-1}
9	Nanosheet on graphene	129 mAh g^{-1} (1 A g^{-1})	76 mAh g^{-1} (20 Ag^{-1})	**50**% from 1 to 20 A g^{-1}

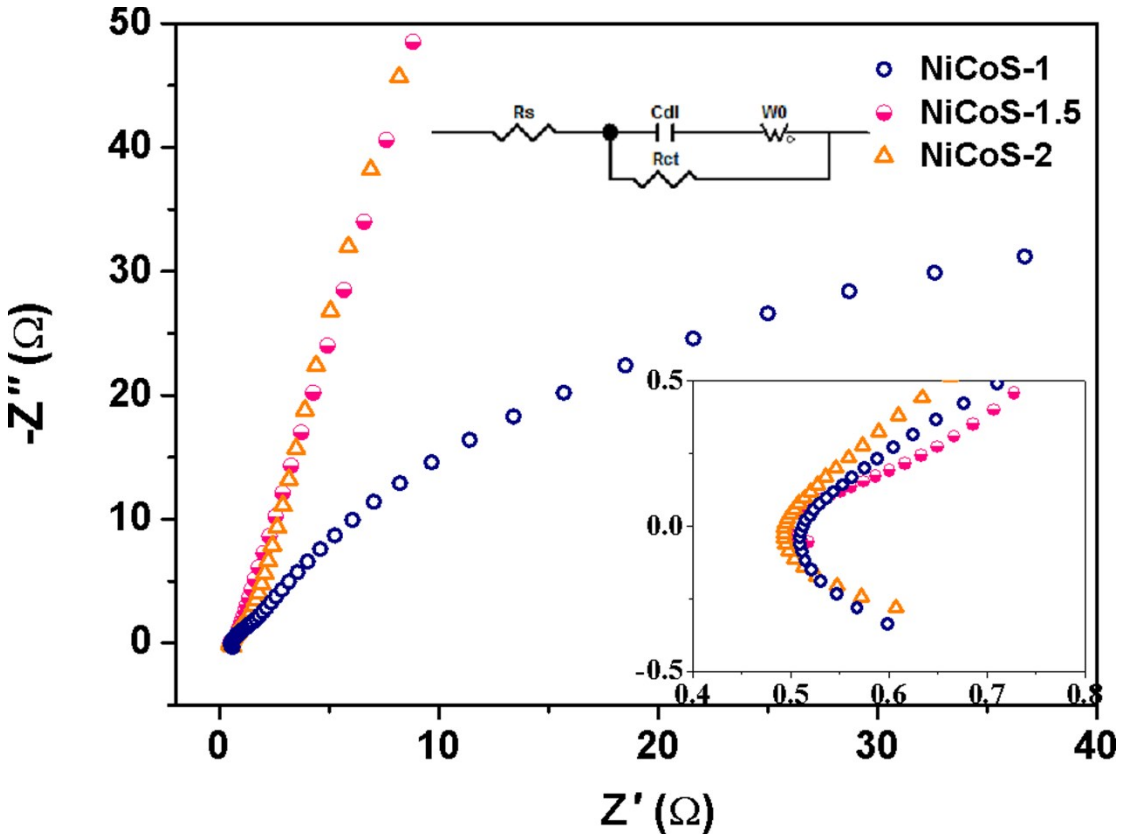

Figure S9. The electrochemical impedance spectra of (a) $NiCo_2S_4$, (b) $Ni_{1.5}Co_{1.5}S_4$, and (c) Ni_2CoS_4.

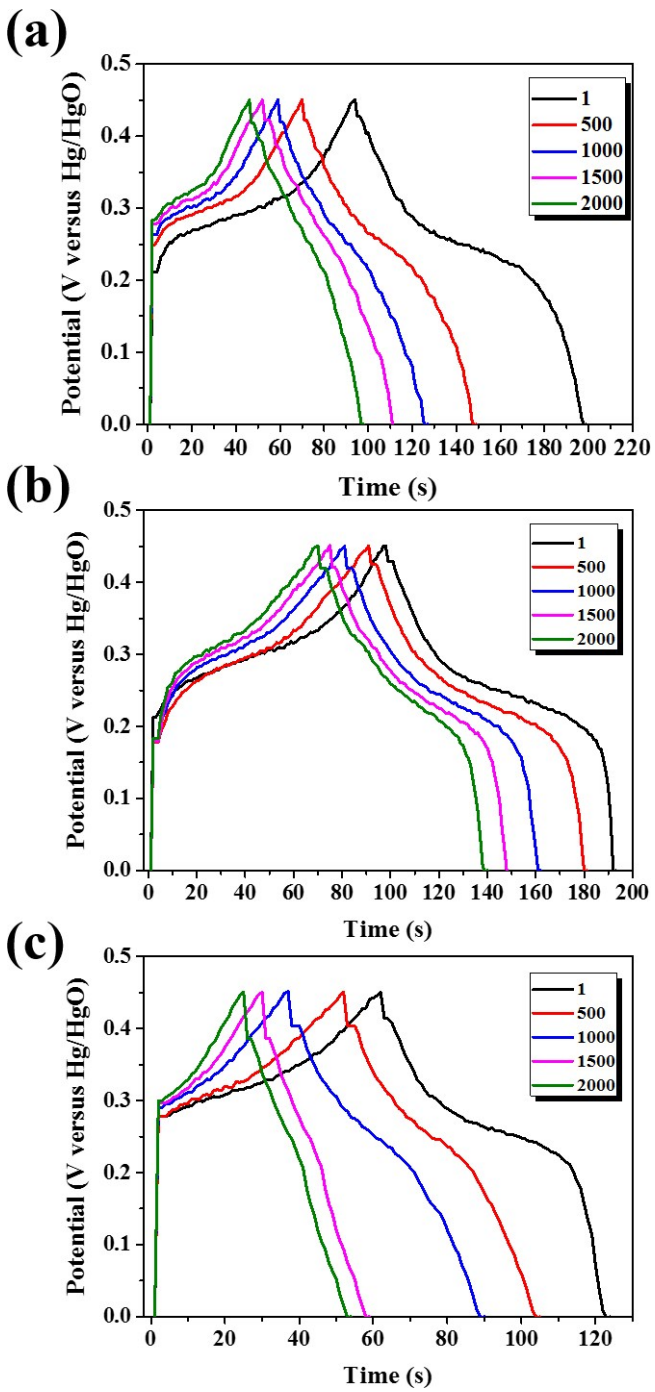

Figure S10. The 1st, 500th, 1000th, 1500th, 2000th charge and discharge cycles of (a) $NiCo_2S_4$, (b) $Ni_{1.5}Co_{1.5}S_4$, and (c) Ni_2CoS_4 during 2000 cycles long-term cycling test.

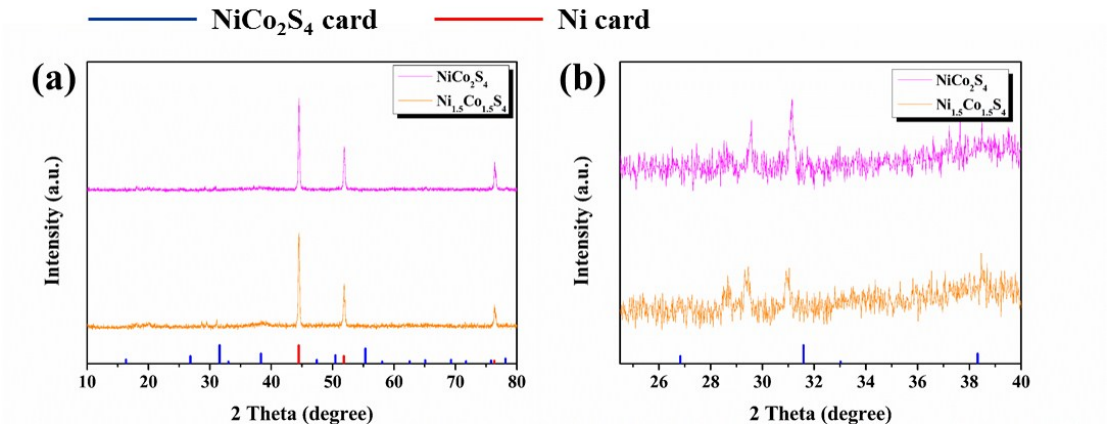

Figure S11. XRD pattern of the nickel cobalt sulfides samples with nickel foam were characterized after 2000 cycles test ranging from (a) 10˚- 80˚, and (b) 24.5˚- 40˚.

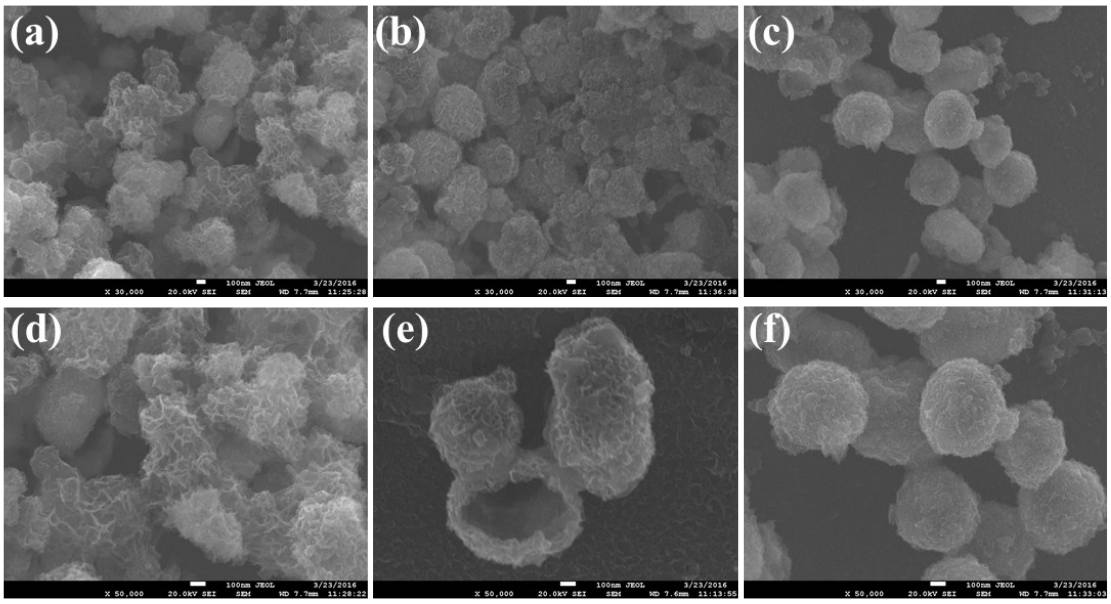

Figure S12. FESEM images of the Ni–Co sulfides: (a, d). $NiCo_2S_4$, (b, e) $Ni_{1.5}Co_{1.5}S_4$, and (c, f) Ni_2CoS_4 after cycling for 2000 cycles at a current density of 5 A g^{-1}, respectively.

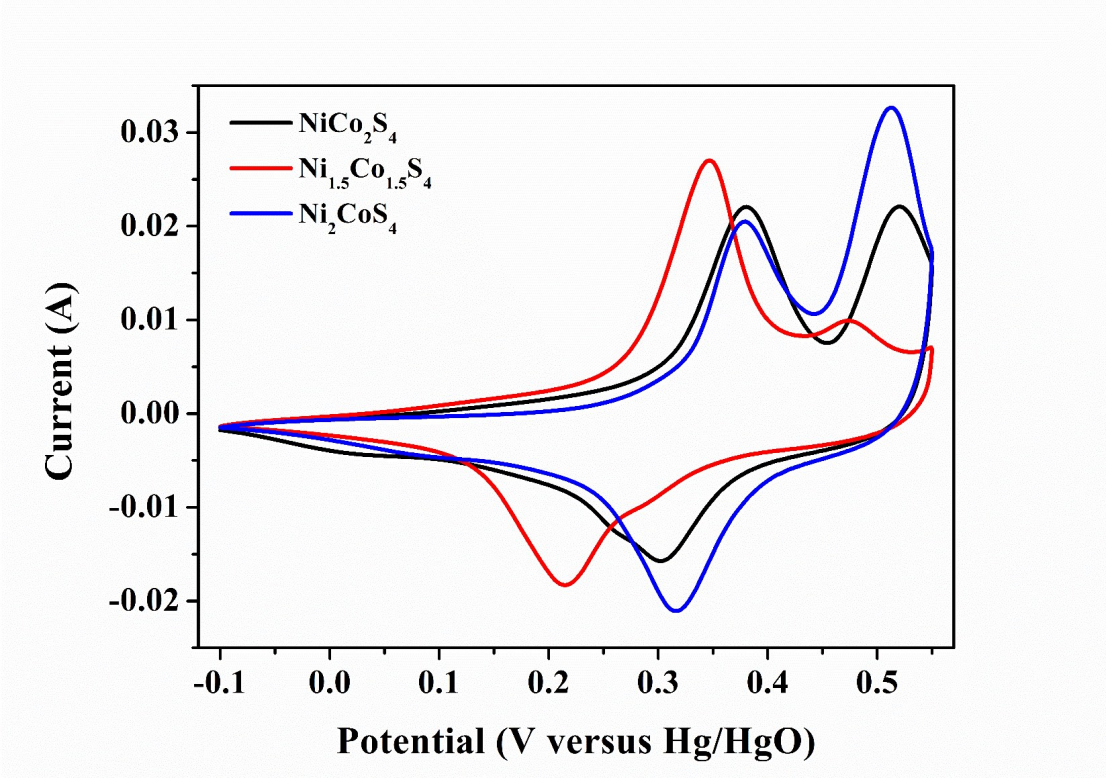

Figure S13. CV curves the nickel cobalt sulfides measured after 2000 charge and discharge cycles.

Supplementary Reference

1. Z. Wu, X. Pu, X. Ji, Y. Zhu, M. Jing, Q. Chen and F. Jiao, *Electrochim Acta*, 2015, **174**, 238-245.
2. L. F. Shen, J. Wang, G. Y. Xu, H. S. Li, H. Dou and X. G. Zhang, *Adv Energy Mater*, 2015, **5**, 1400977-1400984.
3. Y. M. Chen, Z. Li and X. W. Lou, *Angew Chem Int Edit*, 2015, **54**, 10521-10524.
4. X. Xiong, G. Waller, D. Ding, D. Chen, B. Rainwater, B. Zhao, Z. Wang and M. Liu, *Nano Energy*, 2015, **16**, 71-80.
5. L. Yu, L. Zhang, H. B. Wu and X. W. Lou, *Angew Chem Int Edit*, 2014, **53**, 3711-3714.
6. J. Zhang, H. Gao, M. Y. Zhang, Q. Yang and H. X. Chuo, *Appl Surf Sci*, 2015, **349**, 870-875.
7. J. Pu, T. T. Wang, H. Y. Wang, Y. Tong, C. C. Lu, W. Kong and Z. H. Wang, *Chempluschem*, 2014, **79**, 577-583.
8. J. Pu, F. L. Cui, S. B. Chu, T. L. Wang, E. H. Sheng and Z. H. Wang, *Acs Sustain Chem Eng*, 2014, **2**, 809-815.
9. S. J. Peng, L. L. Li, C. C. Li, H. T. Tan, R. Cai, H. Yu, S. Mhaisalkar, M. Srinivasan, S. Ramakrishna and Q. Y. Yan, *Chem Commun*, 2013, **49**, 10178-10180.